

Seismic Response Analysis of Seismically Isolated Buildings with Multilayered Elastomeric Bearings Considering Rocking Behavior

K. Ishii, M. Kikuchi & K. Shirai

Hokkaido University, Sapporo



SUMMARY:

This paper investigates the behavior of seismically isolated buildings with multilayered elastomeric bearings. First, a mechanical model for multilayered elastomeric bearings is proposed to account for changes in the properties of elastomeric bearings that depend on varying axial loadings. Second, analytical models of seismically isolated buildings are generated to simulate the seismic response of isolated buildings. We conduct analyses of isolated structures subjected to steady-state harmonic motion in order to establish a general understanding of their nonlinear responses. Seismic response analyses are also conducted to demonstrate isolated buildings' behavior under severe earthquake excitations. The results obtained from the analyses using a detailed model show that the maximum response acceleration of buildings tends to be limited because their isolators buckle. This buckling behavior may cause the isolators to experience unexpected extra displacement, and the occurrence of buckling suggests that isolators might be severely damaged.

Keywords: Seismic isolation, Multilayered elastomeric bearings, Rocking behavior, Seismic response

1. INTRODUCTION

Seismic isolation is the most effective technology for protecting structures from the damaging effects of earthquakes. It has been used extensively worldwide over the last three decades. The widespread use of seismic isolation has necessitated a better understanding of some of the more complex aspects of isolation device behavior such as that occurring under large shear deformations or high compressive stresses. At large shear deformations, elastomeric bearings exhibit stiffening behavior under low axial stress or buckling behavior under high axial stress. With seismic isolation, buildings can get taller and slenderer, and the imposed compressive stress variations under earthquake excitation can be significant because of rocking behavior. Detailed analytical models that include the influence of rocking behavior enable precise estimation of the dynamic response of seismically isolated structures.

This paper investigates the behavior of seismically isolated buildings with multilayered elastomeric bearings, especially under rocking vibration caused by earthquake excitation. First, a mechanical model for multilayered elastomeric isolation bearings is presented to account for the property changes elastomeric bearings undergo depending on their axial loadings. For the purpose of representing the interaction between shear and axial forces, we use a mechanical model that includes two sets of axial springs, one on the top and the other on the bottom, and a mid-height shear spring, all bound together by rigid columns.

Next, we generate analytical models of seismically isolated buildings to simulate the seismic response of isolated buildings. Isolated buildings are simplified, then their superstructures are modeled as 1 degree of freedom systems supported by three mechanical models of elastomeric bearings, including the influence of varying vertical loads on horizontal hysteretic behavior.

Then we perform two types of response analysis. The first is steady-state vibration analysis under

sinusoidal excitation, and the second is transient response analysis under earthquake ground motion. We investigate the influence of shear-axial interaction on the behavior of isolators by using detailed analytical models of isolated buildings. The results of the analyses show that the maximum restoring force of elastomeric bearings and the maximum acceleration response of superstructures are limited because of buckling behavior of the isolators. These results give us some important suggestions for the safety of seismically isolated structures.

2. A MECHANICAL MODEL FOR MULTILAYERED ELASTOMERIC BEARINGS

2.1. Mechanical Model

Figure 2.1 shows a mechanical model for multilayered elastomeric bearings. This model is proposed to account for property changes that elastomeric bearings exhibit depending on their loading (Kikuchi et al. 2010). Figure 2.2 shows the deformation of the mechanical model under horizontal and vertical loads. To represent the interaction between shear and axial forces, the mechanical model includes two sets of axial springs, one on the top and the other on the bottom and a mid-height multiple shear spring (MSS), all bound together by rigid columns. Each spring in the model is a uniaxial nonlinear spring.

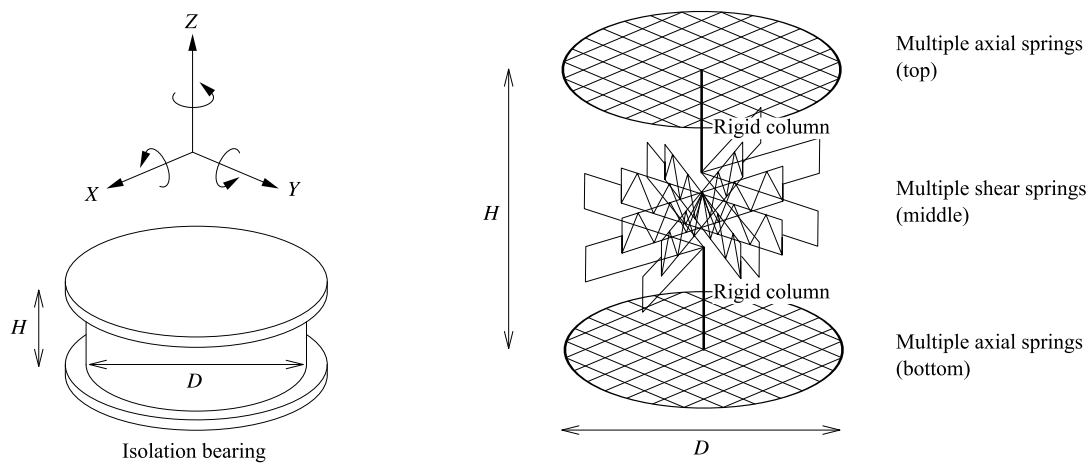


Figure 2.1. Three-dimensional multi-spring mechanical model.

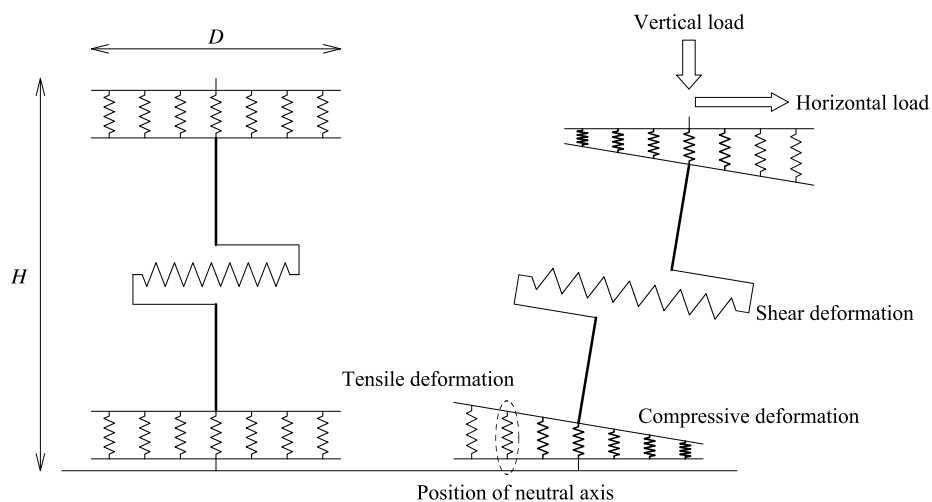


Figure 2.2. Deformation of the mechanical model.

2.1.1. Shear springs

The MSS model, originally proposed to simulate the biaxial behavior of a building (Wada and Hirose

1989), consists of a series of identical shear springs arranged radially (fig. 2.3(a)) to represent the isotropic behavior of multilayered elastomeric bearings in the horizontal plane. In this study, a nonlinear hysteresis model proposed for lead-rubber bearings (LRBs) (Yamamoto et al. 2009) is applied to each shear spring. The hysteresis model can accurately predict the mechanical properties of elastomeric bearings into the large strain range (fig. 2.3(b)).

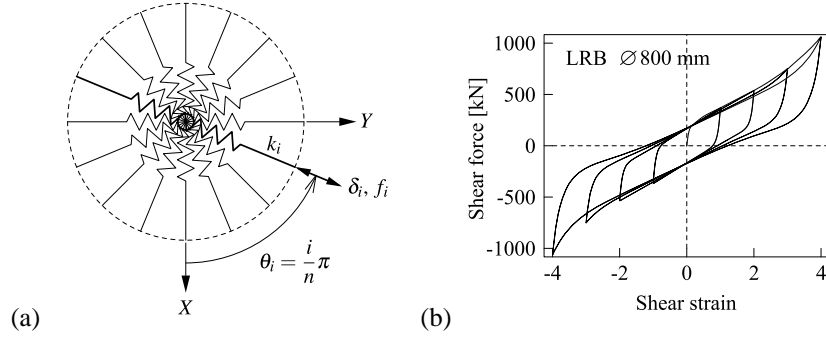


Figure 2.3. Multiple shear springs at mid-height of the model
(a) Diagram of MSS; (b) Shear force-shear strain relationship for the shear springs in the MSS.

2.1.2. Axial springs

Figure 2.4(a) shows a construction of the series of axial springs at the top and bottom of the mechanical model. Each axial spring represents an individual fiber of the bearing's cross-sectional area. Figure 2.4(b) shows the stress-strain relationship for the axial springs (Kikuchi et al. 2010). This hysteresis model accounts for the nonlinear vertical behavior of multilayered elastomeric bearings. Multilayered elastomeric bearings consist of many rubber layers whose top and bottom surfaces are bonded to steel plates to restrict compressive deformation. The deformation constraints provide compressive modulus distribution over the cross section of the rubber layers. This compressive modulus distribution is considered in the proposed mechanical model (fig. 2.5). The initial compression modulus, E_{init} , of each spring can be calculated from the following equations (Ishii et al. 2011):

$$E_{init} = K \left\{ 1 - \frac{I_0(\lambda r/R)}{I_0(\lambda)} \right\} \quad (2.1)$$

$$\lambda = 4S_1 \sqrt{\frac{3G}{K}} \quad (2.2)$$

where S_1 is the shape factor of the rubber layer, G is the shear modulus of rubber, K is the bulk modulus of rubber, R is the radius of the rubber, r is the distance of each spring from the center of the rubber, and I_0 is the modified Bessel function of the first kind of order 0.

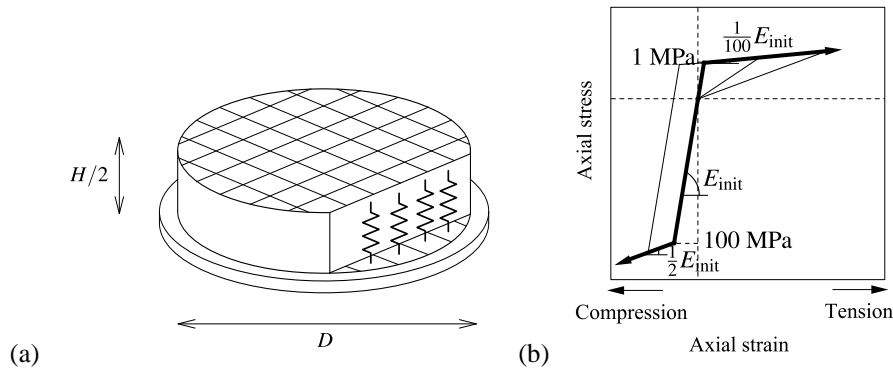


Figure 2.4. Multiple axial springs at the top and bottom of the model
(a) Diagram of multiple axial springs; (b) Axial stress-axial strain relationship for multiple axial springs.

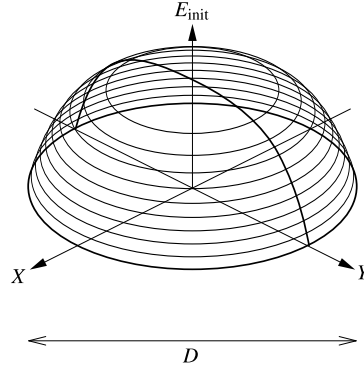


Figure 2.5. Distribution of initial compression modulus.

2.2. Hysteresis Loops under Various Vertical Loads

Figure 2.6 shows the results of the analysis of simulated LRB cyclic loading tests using the mechanical model. At large shear deformations, the hysteresis loop shows stiffening behavior under low axial stress or buckling behavior under high axial stress. These mechanical property changes are generally accepted for the nonlinear behavior of elastomeric isolation bearings.

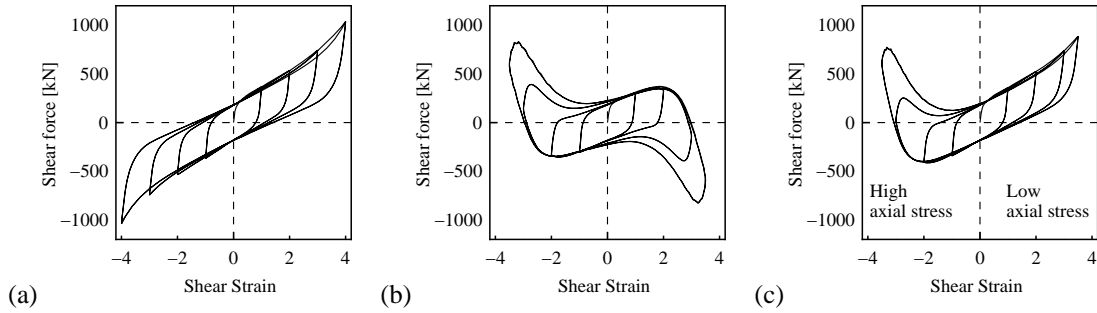


Figure 2.6. Shear force-shear strain hysteresis loops:
(a) under 1 MPa compressive stress; (b) 20 MPa; (c) 0 to 20 MPa (varies with shear deformation).

3. ANALYTICAL MODEL FOR SEISMICALLY ISOLATED BUILDINGS

In this section, we describe analytical models of seismically isolated buildings. These models are used in section 4 to simulate the seismic response of isolated buildings. A seismically isolated building used in the modelling is shown in fig. 3.1. The building is modelled as a 1-degree of freedom (DOF) system supported by three isolators. Stiffness proportional damping of the superstructure is assumed, with a damping ratio of 2% of critical at the fundamental period of the fixed-base structure. Fundamental period, T , is estimated as

$$T = 0.02 \times H = 1.2 \text{ [s]} \quad (3.1)$$

where H is the height of the building. When assuming the fundamental mode shape is an inverted triangle, equivalent mass M_e , equivalent height H_e and equivalent stiffness K_e are calculated by the following equations:

$$M_e = \frac{3n+3}{4n+2} M = 1537 \times 10^3 \text{ [kg]} \quad (3.2)$$

$$H_e = \frac{2n+1}{3n} H = 41 \text{ [m]} \quad (3.3)$$

$$K_e = \frac{4\pi^2 M_e}{T^2} = 42.1 \times 10^3 \text{ [kN/m]} \quad (3.4)$$

where M is the total mass of the building and n is the number of stories. The dynamic properties of the building and dimensions of the isolators are shown in Table 3.1 and Table 3.2, respectively. The average compressive pressure on each isolator is 10 MPa.

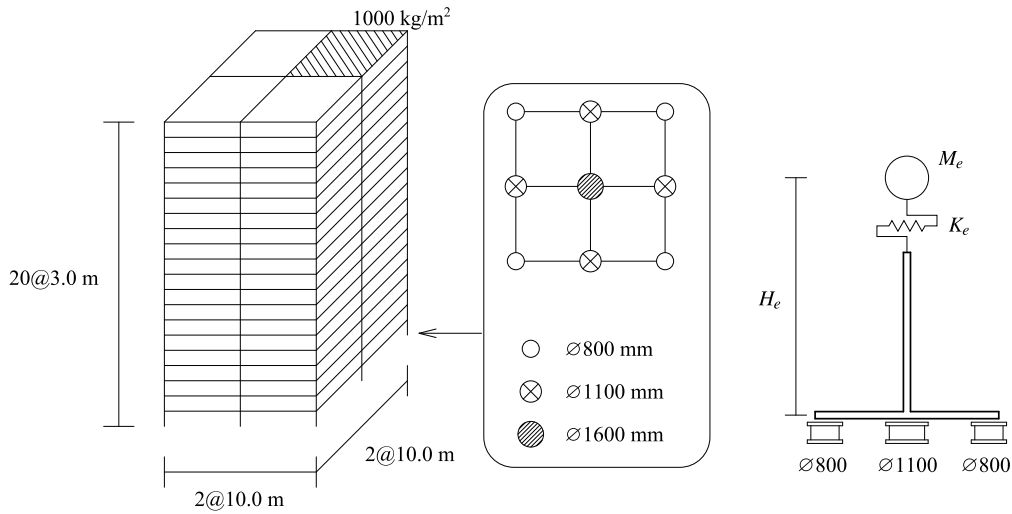


Figure 3.1. Twenty-story reinforced-concrete frame building supported by nine isolators and analytical model.

Table 3.1. Dynamic properties of the building.

	Fixed-base	Isolated
Natural period [s]	1.20	3.38 (equivalent horizontal stiffness at 100% shear strain)
Damping factor	2% (building)	2% (building), 26.5% (isolators)

Table 3.2. Dimensions of LRBs used in analytical models.

Diameter [mm]	Lead plug diameter [mm]	Total rubber thickness [mm]	Shape factor S_1	Aspect ratio S_2
800	160	200 (5 x 40 layers)	40.0	4.0
1100	220	203 (7 x 29 layers)	39.3	5.4

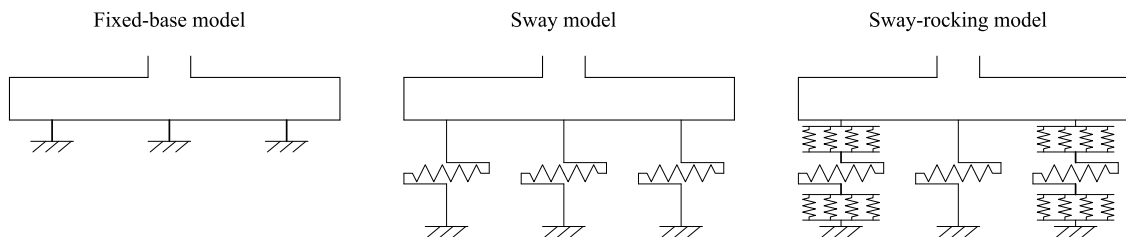


Figure 3.2. Three seismic isolation analytical model types.

Figure 3.2 shows three types of isolator models applied to bearings in the simplified analytical model. The mechanical model expressed in section 2 is used to represent the LRBs and the two other models are also used to help in understanding the effect of varying the vertical load on system response. The first is a fixed-base model, which can simulate the behavior of ordinary buildings. The second is a sway model, which is the same as a 2-DOF model that considers sway motion. This model can simulate the behavior of seismically isolated buildings, but does not include any interaction between the horizontal and vertical forces. The characteristics of isolators are shown in fig. 2.3(b). The third is a sway-rocking model, using the presented mechanical model. This model can include the influence of varying vertical loads on horizontal hysteretic behavior. The characteristics of isolators may change with compressive stress magnitudes during earthquake excitation as shown in fig. 2.6.

4. RESPONSE ANALYSIS

In this section, the influence of varying vertical loads on the behavior of seismic isolation bearings and the influence of this behavior on the response of isolated buildings during earthquake loading are investigated through a series of nonlinear time-history analyses.

4.1. Steady-state Vibration Analysis

We performed numerical analyses subjected to harmonic ground motion of varying frequencies to gain basic insights into the behavior of seismically isolated buildings, taking rocking response into consideration. The time history of harmonic ground acceleration, a_G , is expressed by the following equation:

$$a_G(t) = \alpha S_a(T_G) \times \sin\left(\frac{2\pi}{T_G}t\right) \quad (4.1)$$

$$S_a(T_G) = \begin{cases} 64 + 600T_G & (T_G < 0.16) \\ 160 & (0.16 \leq T_G < 0.64) \\ 102.4/T_G & (0.64 \leq T_G) \end{cases} \quad [\text{cm/s}^2] \quad (4.2)$$

where α is an amplification factor and $2\pi/T_G$ is the frequency of ground motion. S_a is defined as a function of the period T_G to be consistent with the response acceleration spectrum in the Japanese code.

Figure 4.1 shows the relationship between the acceleration response of the superstructure and the period of input ground acceleration in steady-state vibration. Naturally, in the short-period range, the sway model and sway-rocking model produce less response acceleration than the fixed-base model. In the case of $\alpha = 2$, the peak response of sway-locking model is much less than that of sway model. This response reduction is due to the occurrence of the buckling behavior of the isolators. At long-period range, response of the sway-rocking model is larger than the sway model.

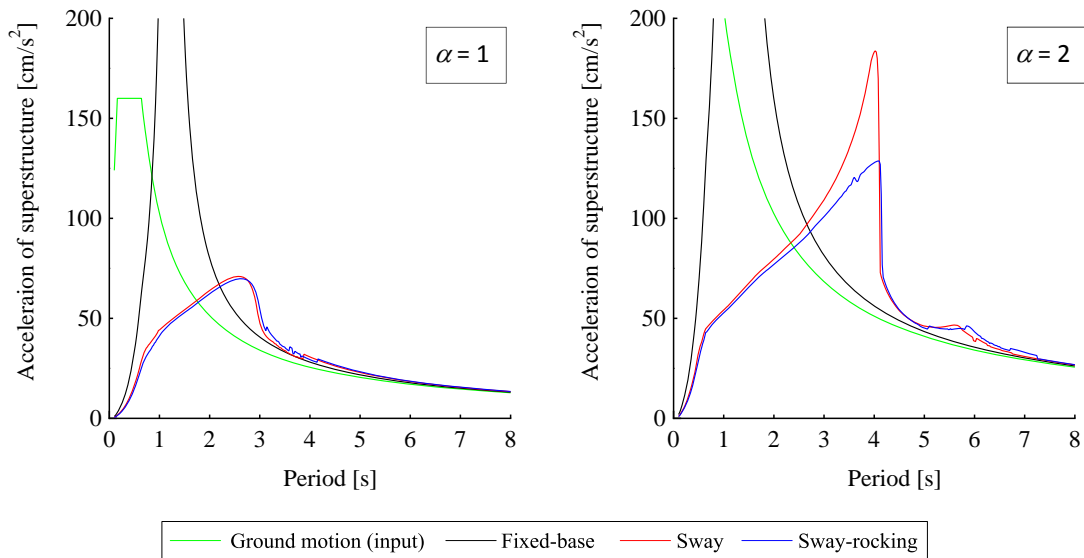


Figure 4.1. Response acceleration of superstructure ($\alpha = 1, 2$).

Figures 4.2 and 4.3 show the response displacement of the superstructure and the isolators. The amplitude of the input ground displacement, S_d , can be calculated by following equation:

$$S_d = S_a / \left(\frac{2\pi}{T_G}\right)^2 \quad (4.3)$$

In the sway model and sway-locking model, the displacement response of the superstructure is a little

larger than that of the isolators, because the superstructure deforms. The trends observed in the response acceleration are also seen in the response displacement.

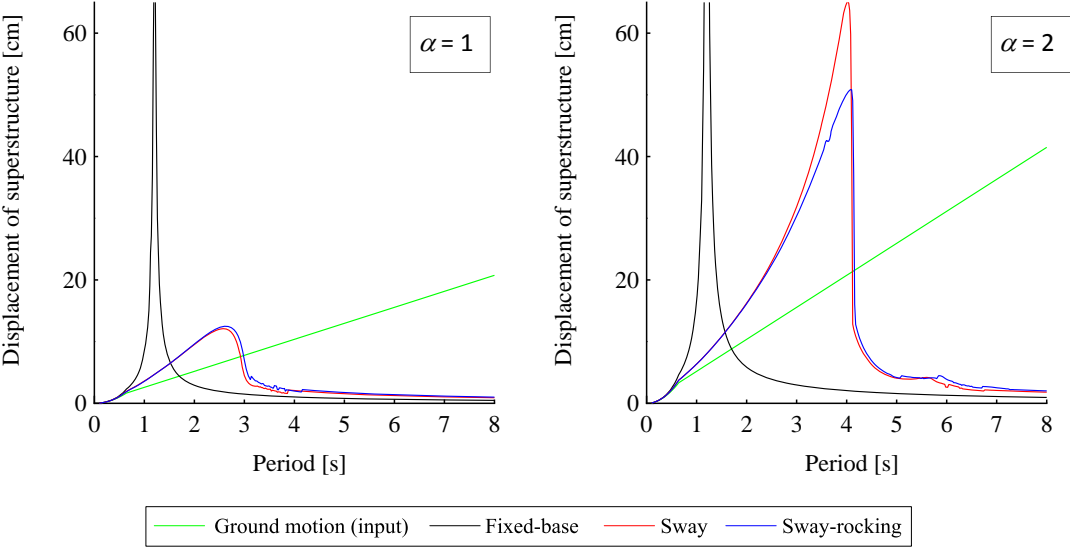


Figure 4.2. Response displacement of superstructure ($\alpha = 1, 2$).

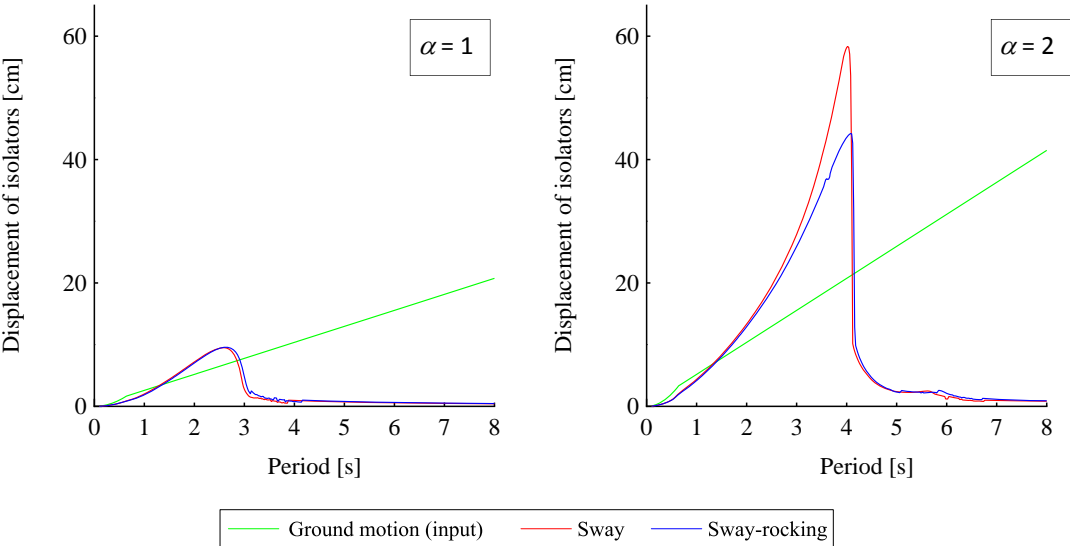


Figure 4.3. Response displacement of isolators ($\alpha = 1, 2$).

Figures 4.4 and 4.5 show shear force-shear displacement hysteresis loops of the isolator at left-side, in the case of $\alpha = 2$, $T_G = 2.0$ and 4.0 . The sway model exhibits symmetrical hysteresis loops, with hardening behavior at $T_G = 4.0$. The sway-rocking model also exhibits a symmetric hysteresis loop at $T_G = 2.0$, however, the hysteresis loop at $T_G = 4.0$ shows asymmetry and buckling behavior is observed in negative displacement range. The asymmetrical hysteresis loop and buckling behavior caused by the variation of axial load under rocking response can be simulated by using the presented mechanical model.

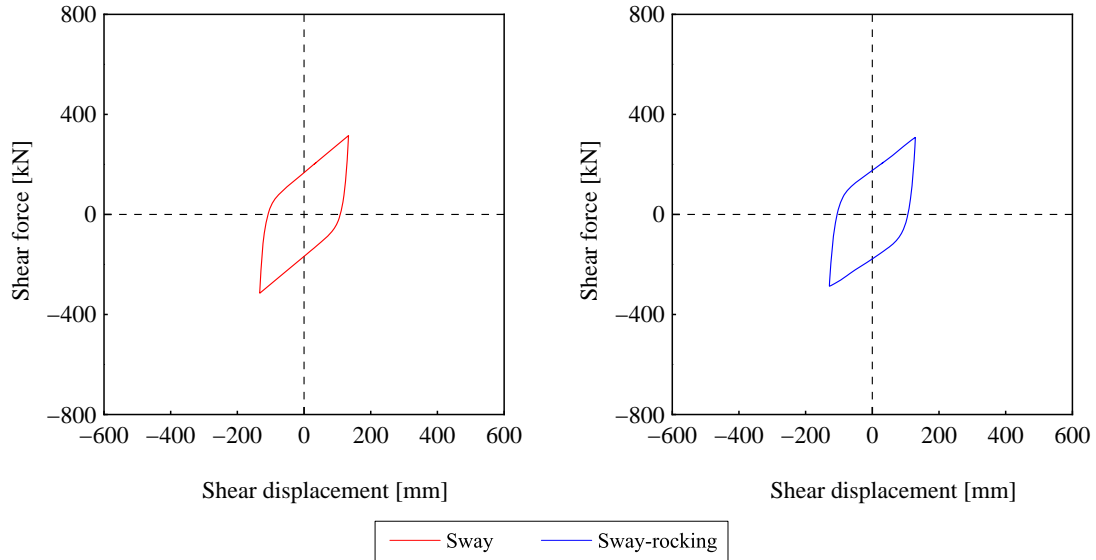


Figure 4.4. Shear force-shear displacement relationship of isolator ($\alpha = 2, T_G = 2.0$).

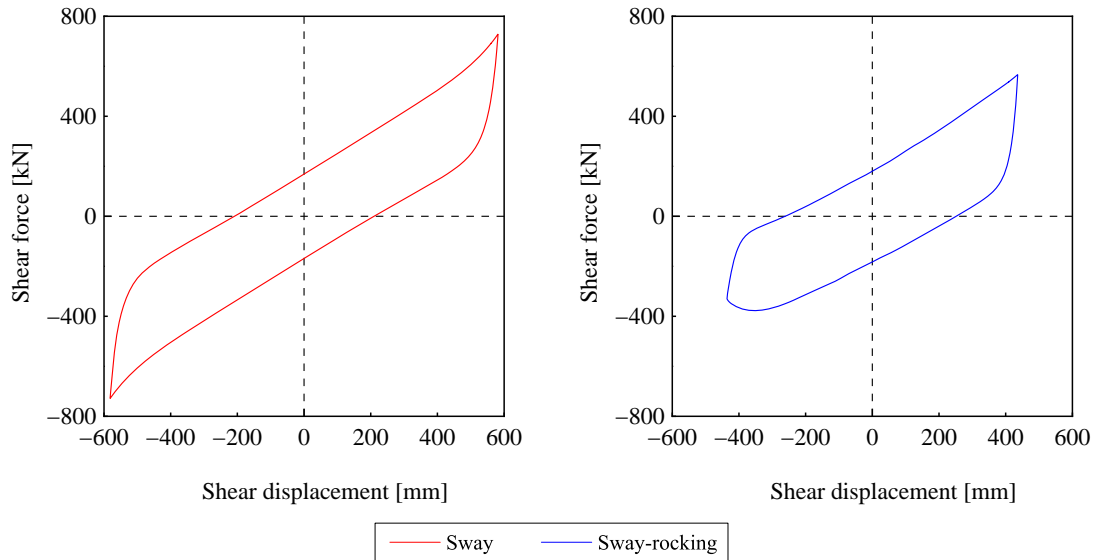


Figure 4.5. Shear force-shear displacement relationship of isolator ($\alpha = 2, T_G = 4.0$).

Under the rocking behavior, an overturning force causes variation of axial force on the right- and left-side isolators. The variation of the axial force, N , which tends to increase with shear displacement, can be estimated by following equation:

$$N = N_0 \pm M_e a \times \frac{H_e}{L} \quad (4.4)$$

where N_0 is the initial axial force, a is the acceleration response of the superstructure (mass point M_e) and L is the distance between the left-side and right-side isolators. Therefore, the amplitude of the variation of axial force is proportional to the amplitude of the response acceleration. In the sway-rocking model, higher axial stress makes the stiffness of the isolators lower, and that lower stiffness causes lower response acceleration. The axial force varies within a limited range, and the progress of isolator buckling tends to be suppressed. This behavior saves isolators from excessive instability.

4.2. Seismic Response Analysis

The well-known historic earthquake ground motion record, 1940 El Centro (E-W), is used for the

transient response analyses. The ground motion is input at three intensities, corresponding to peak ground velocities of 25, 50 and 75 cm/s. The 25 and 50 cm/s velocity levels are generally used as design levels for input ground motion in Japan, and the 75 cm/s velocity is regarded as ultimate level of excitation in this study.

Figure 4.6 shows the maximum response values obtained from the analyses for the three excitation levels. At 25 and 50 cm/s, the sway model and sway-rocking model produce almost identical responses, with the displacement of isolators being not more than 30 cm (corresponding to a shear strain of 150%). In the ultimate excitation level, the response acceleration of the sway-rocking model is about 20% lower than that of the sway model, because the isolators buckle.

Figure 4.7 shows the force-displacement relationship of the left-side isolator at the 75 cm/s excitation level. The maximum restoring force in the negative displacement of the sway-rocking model is 400 kN, about 60% of that of the sway model. This hysteresis loop shows buckling behavior with a maximum compressive pressure of 19 MPa. This buckling behavior may cause unexpected extra displacement of the isolators, and suggests that the isolators might be severely damaged.

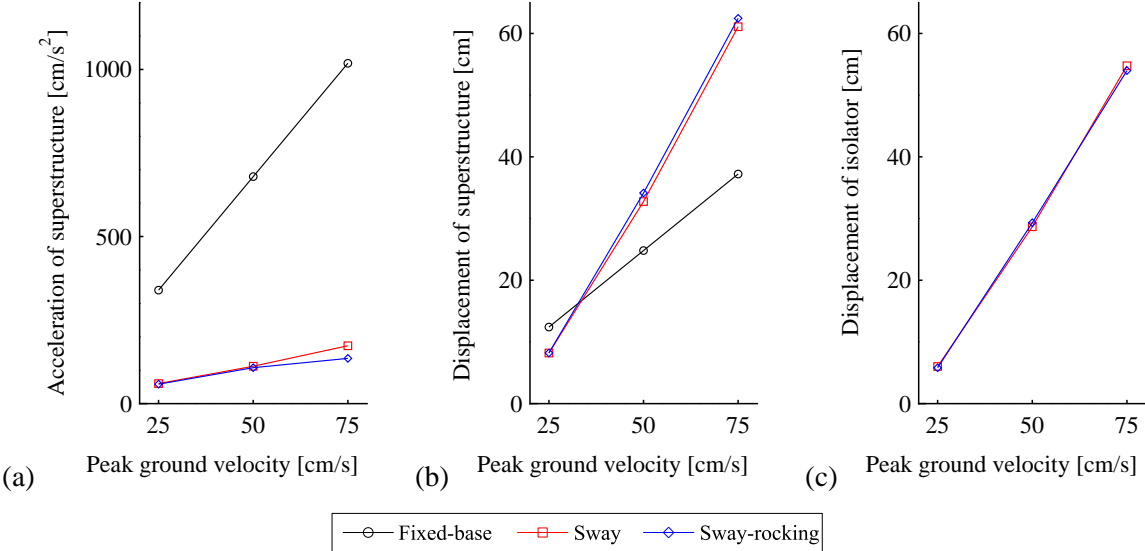


Figure 4.6. Maximum response values obtained from the seismic response analyses (a) Acceleration of superstructure; (b) Displacement of superstructure; (c) Displacement of isolators.

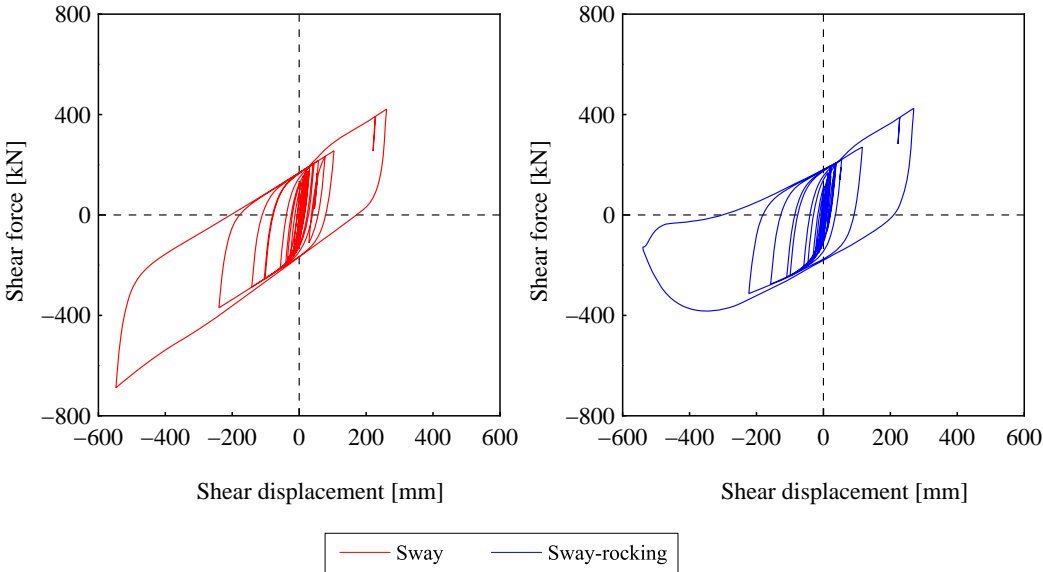


Figure 4.7. Force-displacement relationship of the left-side isolator (75 cm/s excitation level).

5. CONCLUSIONS

This paper has investigated the behavior of seismically isolated buildings with multilayered elastomeric bearings, especially under rocking vibration caused by earthquake excitation. The conclusions are as follows.

First, we presented a mechanical model for multilayered elastomeric isolation bearings. The model includes the interaction between shear and axial forces, and can represent the characteristic changes of isolators experiencing varying axial forces during earthquake excitation.

Next, we produced an analytical model for seismically isolated buildings. The detailed sway-rocking model uses the presented mechanical model and can express the rocking behavior of seismically isolated buildings. Rocking behavior produces axial force variation on the isolators, and severe axial force may cause buckling. Detailed modeling considering rocking behavior is more important for taller isolated buildings, because the axial force variation on the isolators tends to be more significant in such structures.

Finally, we present response analyses, one being a steady-state vibration analysis under sinusoidal excitation and the other being a transient response analysis under earthquake ground motion. We investigated the influence of shear-axial interaction on the behavior of the isolators by using the analytical model for isolated buildings. The results obtained from the detailed sway-rocking model differ from those given by the simple sway model under severe excitation. Using the sway-rocking model, the maximum response acceleration of the superstructure tends to be limited because of buckling of the isolators. This buckling may cause unexpected extra displacement of the isolators, and suggests that the isolators are severely damaged. Consideration should be given to the buckling behavior caused by severe axial loads for more accurate prediction of the response of these types of seismically isolated buildings.

ACKNOWLEDGEMENT

Part of our numerical analysis results was obtained using an analytical program developed by Shimizu Corporation. The authors would like to express their thanks for its contributions.

REFERENCES

- Kikuchi M, Nakamura T. and Aiken I. D. (2010). Three dimensional analysis for square seismic isolation bearings under large shear deformations and high axial loads. *Earthquake Engineering and Structural Dynamics*. **39**. 1513–1531.
- Wada A. and Hirose K. (1989). Building frames subjected to 2D earthquake motion. *Proceedings, Structure Congress '89*. ASCE. San Francisco, CA. 388–397.
- Yamamoto S., Kikuchi M., Ueda M. and Aiken I. D. (2009). A mechanical model for elastomeric seismic isolation bearings including the influence of axial load. *Earthquake Engineering and Structural Dynamics*. **38**. 157–180.
- Ishii K., Kitayama S. and Kikuchi M. (2011). An analytical model for seismic isolation bearings under large shear deformations including the influence of compression modulus distribution. *Summaries of Technical Papers of Annual Meeting. AIJ*. **B-2**. 523–526.